

Tumor suppressor miR-520a inhibits cell growth by negatively regulating PI3K/AKT signaling pathway in acute myeloid leukemia

*Jing Xiao^{1,A–C,E,F}, *Fang Wan^{2,A,C,E,F}, Lin Tian^{1,A,C–F}, Yao Li^{1,A,C,F}

¹ Department of Pathology, Renmin Hospital, Hubei University of Medicine, Shiyan, China

² Department of Pediatrics, Renmin Hospital, Hubei University of Medicine, Shiyan, China

A – research concept and design; B – collection and/or assembly of data; C – data analysis and interpretation;

D – writing the article; E – critical revision of the article; F – final approval of the article

Advances in Clinical and Experimental Medicine, ISSN 1899–5276 (print), ISSN 2451–2680 (online)

Adv Clin Exp Med. 2024;33(7):729–738

Address for correspondence

Yao Li

E-mail: leo9029@sina.com

Funding sources

None declared

Conflict of interest

None declared

*Jing Xiao and Fang Wan contributed equally to this work.

Received on March 23, 2023

Reviewed on April 10, 2023

Accepted on August 16, 2023

Published online on October 19, 2023

Abstract

Background. Short regulatory RNAs, called microRNAs (miRNAs), have been found to possess regulatory functions in cancer and, as such, have recently been evaluated for their therapeutic role against various human malignancies.

Objectives. The present work aimed to investigate whether miR-520a can play a therapeutic role in the treatment of human acute myeloid leukemia.

Materials and methods. Human myeloid leukemia cell lines (Kasumi-1, Kasumi-3, Kasumi-6, BDCM, and K562) and a normal myeloid cell line (NCI-H5N6) were used for the study. Cell lines were subjected to real-time quantitative polymerase chain reaction (RT-qPCR), evaluation of cell viability and proliferation by MTT assay and colony formation assays. Dual acridine orange (AO)/ethidium bromide (EB) staining was applied for transfected K562 cells with miR-negative control (NC) or miR-520a mimics, and annexin V-fluorescein isothiocyanate (FITC)/propidium iodide (PI) dual staining and flow cytometry were performed to analyze cancer cell apoptosis followed by western blot.

Results. Cancerous cell lines exhibited lower gene expression of miR-520a, and its overexpression significantly reduced ($p < 0.05$) the proliferation and viability of cancer cells. Cancer cells demonstrated the induction of Bax/Bcl-2-mediated apoptosis following miR-520a overexpression. The miR-520a was shown to target the PI3K/AKT signaling pathway in human acute myeloid leukemia to exercise its regulatory role in cancer.

Conclusions. The study showed that miR-520a actively regulated cell proliferation in acute myeloid leukemia and illustrated the mechanism by which it exerts its regulatory role, emphasizing the possibility of targeting miR-520a as an efficient therapeutic strategy against human acute myeloid leukemia.

Key words: microRNA, cell proliferation, AO/EB staining, apoptosis, acute myeloid leukemia

Cite as

Xiao J, Wan F, Tian L, Li Y. Tumor suppressor miR-520a inhibits cell growth by negatively regulating PI3K/AKT signaling pathway in acute myeloid leukemia. *Adv Clin Exp Med.* 2024;33(7):729–738. doi:10.17219/acem/171299

DOI

10.17219/acem/171299

Copyright

Copyright by Author(s)

This is an article distributed under the terms of the Creative Commons Attribution 3.0 Unported (CC BY 3.0) (<https://creativecommons.org/licenses/by/3.0/>)

Background

There are many types of leukemia, but acute leukemia is one of the most common hematologic malignancies. It has been shown that acute leukemia occurs due to the abnormal proliferation of hematopoietic stem cells in the bone marrow and other hematopoietic tissues. Moreover, malignant cells have also been shown to accumulate in these tissues.¹ Acute myeloid leukemia results in impaired blood cell production and bone marrow failure.² If left untreated, patients with this disorder can die in a few weeks due to increased susceptibility to blood infections or uncontrolled blood loss caused by excessive bleeding.³ Acute leukemia is generally classified as either acute lymphoblastic leukemia (ALL) or acute myeloid leukemia (AML), according to its distinctive morphology, prognosis and preferred treatment protocols to differentiate them.⁴ Among hematopoietic disorders, AML is characterized by the presence of numerous cytogenetic and molecular abnormalities,^{5,6} and there are high morbidity and mortality rates associated with AML when compared to other cancers. The main therapeutic strategies used in the treatment of AML are chemotherapy and allogeneic stem cell transplantation.⁷ However, in general, the 5-year survival rate of patients with AML is still unsatisfactory.⁸ Therefore, the etiology of the disease needs to be investigated, and new therapeutic strategies must be formulated.

Several studies have shown that microRNA (miR) has an important role to play in regulating the expression of genes by the regulation of post-translational expression. Furthermore, miRs may play a role in the progression of a significant number of diseases.⁹ According to recent studies, miRNAs are involved in the regulation of leukemia progression, including both AML and chronic myeloid leukemia (CML).¹⁰ The miR-520a controls the growth and progression of many human cancers.¹¹ A recent study has demonstrated that miR-520a suppresses the progression of non-small cell lung cancer by targeting the RRM2/Wnt pathway.¹² Based on investigations carried out in HCT116 and SW480 cells, silencing of ATAD2 modulates vascular endothelial growth factor A (VEGFA) and miR-520a in colorectal cancer.¹³ Moreover, a study found that miR-520a regulates endoplasmic reticulum (ER) stress, proliferation, and the AKT1/NF- κ B or PERK/eIF2 signaling pathways in Raji cells.¹⁴ Another study showed that piperine significantly decreased analgesia in the rat model without compression of the lumbar disc herniation by specifically and directly targeting P65 with miR-520a to treat sciatica.

However, the regulatory function of miR-520a in AML is scarce, which prompted us to evaluate the potential underlying molecular mechanisms. Furthermore, in this study, we present the therapeutic benefits of miR-520a in activating the PI3K/AKT signaling pathway for AML and suggest that targeting miR-520a could be an effective anticancer strategy against this disease.

Objectives

We aimed to investigate whether miR-520a can play a therapeutic role in the treatment of human AML by activating the PI3K/AKT signaling pathway.

Materials and methods

Tissue samples

Samples of blood from both AML patients (24 samples) and healthy controls (22 samples) were collected from Renmin Hospital (Hubei University of Medicine, Shiyan, China) between August 2019 and September 2020. The healthy control samples were collected from normal blood donors. There was no chemotherapy or radiation therapy administered to these patients prior to sample collection, and there was no evidence of infections or multiple cancers, indicating that there was no history of multiple cancers among these patients. Patient and healthy control demographics are outlined in Table 1. All patients signed an informed consent form before the procedure. The study was approved by the Ethics Committee of Renmin Hospital (protocol No. FPH-34/2341/22), and the experimental procedure was carried out in accordance with the principles of the Declaration of Helsinki.

Cell lines

Human myeloid leukemia cell lines (Kasumi-1, Kasumi-3, Kasumi-6, BDCM, and K562) and a normal myeloid cell line (NCI-H5N6) were obtained as donations from the Department of Hematology of the Third Hospital of Shanxi Medical University (Taiyuan, China). Cell lines were cultured in RPMI-1640 medium (Invitrogen, Carlsbad, USA), containing 10% fetal bovine serum (FBS) in 5% CO₂ at 37°C. Plasma cells were isolated and cultured from peripheral blood smears according to previously published methods.¹⁵ A colorimetric detection method (InvivoGen, San Diego, USA) was used to identify mycoplasma contamination in cell cultures, and the used cell cultures were free of mycoplasma contamination.

Cell transfection

The cells were seeded in 6-well plates at a density of 3×10^5 cells per well. According to our previous report, 5 μ L of miRNA (miR-negative control (NC) or miR-520a mimics, 50 nM; Thermo Fisher Scientific, Waltham, USA) were transfected into K562 cells during the logarithmic growth phase using HiPerFect Transfection Reagent (5 μ L in 300 μ L of Dulbecco's modified Eagle medium (DMEM); QIAGEN, Germantown, USA) without serum, and incubated at 37°C for 20 min following the manufacturer's instructions. The cells were cultured in a CO₂ incubator

Table 1. Demographics and clinical characteristics of patients and healthy blood donors

Variables	Characteristics											
	healthy volunteers (control or normal, n = 22)			AML patients (n = 24)			Mann–Whitney U			p-value		
	total (n = 22)	male (n = 15)	female (n = 7)	total (n = 24)	male (n = 18)	female (n = 6)	total	male	female	total	male	female
Age at diagnosis [years]												
Minimum	45.00	45.00	48.00	47.00	51.00	47.00	203	96	12	0.3655	0.2395	0.4293
Q1	48.75	48.00	49.00	54.50	55.00	48.00						
Median	55.50	56.00	53.00	57.00	57.00	49.00						
Q3	62.25	62.00	64.00	63.00	63.00	60.00						
Maximum	67.00	67.00	66.00	68.00	68.00	63.00						
Peripheral blasts [%]												
Minimum	–	–	–	37.00	37.00	40.10	–	–	–	–	–	–
Q1	–	–	–	40.93	41.50	40.65	–	–	–	–	–	–
Median	–	–	–	47.50	56.00	41.50	–	–	–	–	–	–
Q3	–	–	–	60.25	68.00	42.20	–	–	–	–	–	–
Maximum	–	–	–	78.00	78.00	42.30	–	–	–	–	–	–

AML – acute myeloid leukemia; Q1 – 1st quartile; Q3 – 3rd quartile. In healthy volunteers, there were usually no blast cells in the blood.

Table 2. Primers used in the study

Gene	Primers	Annealing temperature [°C]
miR-520a	forward: 5'-CCTAACAACCCGTTGCCCTTCTTT-3' reverse: 3'-ACGTGACGGTGGCCAGGT-5'	53
U6	forward: 5'-CTGCCCTTGCCGAGCAAC-3' reverse: 5'-AAGCTCTTACGATAATTGCCT-3'	54
β-actin	forward: 5'-TGCCGAACCATTACCTACAA-3' reverse: 5'-ACCAGAGGATAACAGAGGGATG-3'	58

for 24 h at 37°C to determine whether the transgene was expressed in cells.

In this study, a control plasmid containing empty sequences was used as a control. All plasmids were obtained from Invitrogen.

Real-time PCR

We used an Agilent High Sensitivity RNA Screen Tape (Agilent Technologies, Santa Clara, USA) as a tool to determine the quality of the RNA. The RNA was subjected to reverse transcription as soon as it was isolated from cells.¹⁶

Total RNA was extracted using TRIzol reagent to conduct RNA analysis in clinical samples and cell lines. This was done by following the manufacturer’s instructions. To quantify the level of miR-520a transcript, DNase I was used to remove any DNA contamination, and approx. 1 µg of purified RNA was used to produce complementary DNA (cDNA) using an iScript™ cDNA Synthesis Kit (Bio-Rad, Hercules, USA). Real-time polymerase chain reaction (PCR) was then performed using the SYBR Green Master mix (Thermo Fisher Scientific, Waltham, USA). Three replicates were used for each real-time reaction, and the relative expression levels were quantified using

the 2^{–ΔΔCt} method. Human β-actin was used as an internal control for miR-520a expression. Primers (Table 2) were synthesized by Suzhou Ruibo Biotechnology Co., Ltd. (Guangzhou, China).

MTT proliferation assay

The proliferation of K562 cancer cells, transfected with miR-NC or miR-520a mimics using Lipofectamine 2000 (Thermo Fisher Scientific), was estimated by the MTT assay. In brief, transfected K562 cancer cells (2×10⁵ per well) were placed in a 96-well plate, then cultured in RPMI-1640 medium for 0, 12, 24, 48, or 96 h at 37°C. Each well had 10 µL of MTT reagent (dissolved in phosphate-buffered saline (PBS) (5 mg/mL)) added, followed by prolonged incubation for 4 h at 37°C. The culture medium was removed and dimethyl sulfoxide (DMSO) (150 µL) was added to each well. Then, the samples were processed for absorbance measurement at 570 nm to examine cell proliferation rates.¹⁶

Colony-forming assay

Following its transfection with miR-NC or miR-520a mimics, each 6-well plate was filled with 100 µL

of homogeneous K562 cellular mix in RPMI-1640 medium. The plate was incubated for 10 days at 37°C. Subsequently, the cell cultures were harvested, rinsed 3 times with PBS, and then fixed and stained in ethanol (70%) with crystal violet (0.1%) (Abcam, Waltham, USA). The cells were examined under a microscope, and the relative colony number was presented as a percentage value. Two independent researchers (blind) counted colonies with >50 cells using a low-resolution bright field microscope (Olympus, Tokyo, Japan). A scan of each plate was also analyzed using colony counting software (ImageJ; National Institutes of Health, Bethesda, USA) to automatically detect colonies.¹⁶

Acridine orange/ethidium bromide staining

The K562 cells (2×10^5 cells) with miR-NC or miR-520a mimics to stimulate miRNA expression were seeded in the 12-well plate. The cells were harvested after 24 h of culture at 37°C and washed twice with PBS. Then, they were fixed with methanol, and dual staining with acridine orange/ethidium bromide (AO/EB) (Cat No. E607308; Sangon Biotech Co., Ltd., Shanghai, China) was applied. A fluorescent microscope (Olympus Corp., Tokyo, Japan) was used to analyze their nuclear morphology.¹⁶

Annexin V-FITC/PI dual staining and flow cytometry

Flow cytometry was performed to assess cell apoptosis. Briefly, miR-NC or miR-520a mimics were transfected and 2×10^6 cells per well were cultured for 48 h in a 12-well plate. The K562 cells were incubated at 37°C for 2 h with 10 μ L of fluorescein isothiocyanate (FITC) and 5 μ L of propidium iodide (PI) (Beyotime, Nanjing, China). After centrifugation and washing with PBS, the cells were harvested and fixed in ethanol. Then, the apoptosis was detected by flow cytometry (BD Biosciences, San Diego, USA), following the manufacturer's instructions. Apoptotic subpopulations were differentiated as follows: early apoptosis (Annexin V+/PI-), late apoptosis (Annexin V+/PI+), or necrotic/dead (Annexin V-/PI+). A total of 10,000 cells were analyzed per replicate.¹⁶

Western blot

The K562 cells transfected with miR-NC or miR-520a mimics were lysed with ice-cold radioimmunoprecipitation assay (RIPA) lysis buffer (Sigma-Aldrich, St. Louis, USA), and the total protein concentration was measured using a bicinchoninic acid (BCA) protein assay kit (Sigma-Aldrich). To analyze the protein of each sample, 30 μ g of protein from each sample was separated on a 10% sodium dodecyl-sulfate polyacrylamide gel electrophoresis (SDS-PAGE) gel (Bio-Rad Laboratories

Co., Ltd., Shanghai, China) before being transferred to polyvinylidene difluoride (PVDF) membranes (Millipore, Burlington, USA). Primary antibodies used are as follows: Bcl2 (Cat. No. MA5-11757, dilution 1:800; Thermo Fisher Scientific), Bax (Cat. No. MA5-14003, dilution 1:800; Thermo Fisher Scientific), PI3K (Cat. No. A27091, dilution 1:1000; Invitrogen), Phospho-PI3K (Cat. No. PA5-17387, dilution 1:1000; Invitrogen), AKT (Cat. No. A25810, dilution 1:1000; Antibodies, Cambridge, UK), and Phospho-AKT (Cat. No. A27292, dilution 1:800; Antibodies). The PVDF membranes were blocked with 10% fat-free milk in Tris-buffered saline/Tween-20 (TBST) and incubated with the primary antibodies for 3 h at room temperature. Then, a goat anti-rabbit horseradish peroxidase (HRP) conjugated secondary antibody (dilution 1:8000; Thermo Fisher Scientific) was incubated with the PVDF membranes for 2 h at room temperature. The bands were detected and photographed using a chemiluminescence analyzer (Biotech Co., Ltd., Beijing, China). A densitometric analysis of protein bands was performed using Quantity One software (Bio-Rad) with samples normalized to β -actin.¹⁶

Statistical analyses

GraphPad Prism (v. 9.1; GraphPad Software, Boston, USA) was used to analyze the data, and a minimum of 3 or 5 independent replications were carried out for each experiment ($n = 3-5$). The Mann-Whitney U test was performed with respect to age and sex distribution and peripheral blast (PB) count. The Shapiro-Wilk normality test and Kolmogorov-Smirnov test were performed to determine whether the data conformed to a normal distribution. We found that the data were non-normally distributed. Therefore, data are presented as a median with an interquartile range (Q1-Q3). The Mann-Whitney U test was employed to compare 2 groups, and the Kruskal-Wallis test, followed by Dunn's multiple comparison test were used for comparing multiple groups. A value of $p < 0.05$ was considered statistically significant.

Results

The expression of miR-520a is negatively regulated in AML

Real-time PCR expression analysis was used to investigate the relative expression of miR-520a in tissue samples. We found that miR-520a displayed significantly reduced expression in cancerous tissues compared to normal bone marrow tissue specimens (Fig. 1A, Table 3; $p < 0.0001$; Mann-Whitney test, $U = 75.5$). Similarly, cancer cell lines showed a substantially lower expression of miR-520a transcripts compared to the normal myeloid cell line (Fig. 1B, Table 4; $p = 0.0004$; Kruskal-Wallis test followed by Dunn's

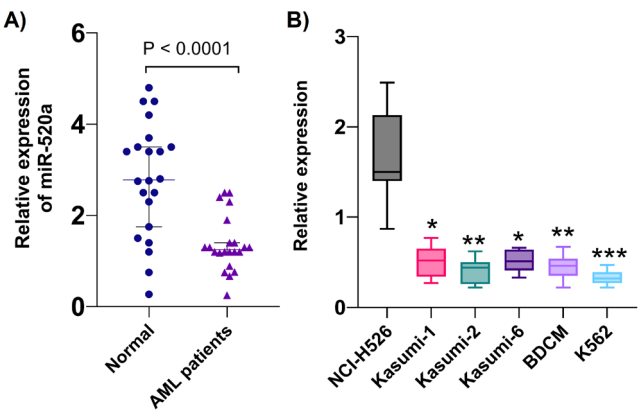


Fig. 1. MicroRNA (miR)-520a is downregulated in acute myeloid leukemia (AML). **A.** Real-time quantitative polymerase chain reaction (RT-qPCR) analysis of miR-520a in tissue specimens of AML patients and healthy volunteers. The data were not normally distributed and were tested by the Shapiro–Wilk test and Kolmogorov–Smirnov test with p-values for healthy control ($p = 0.023$; $p = 0.013$) and AML patients ($p = 0.037$; $p = 0.021$). The Mann–Whitney test was used to compare the 2 groups. The data are presented as a median with interquartile range (Q1–Q3); **B.** RT-qPCR analysis in normal myeloid cells (NCI-H5N6) and various myeloid cancerous cell lines. The data were not normally distributed and were tested by the Shapiro–Wilk test and Kolmogorov–Smirnov test with p-values for NCI-H526 ($p = 0.032$; $p = 0.0152$), Kasumi-1 ($p = 0.027$; $p = 0.021$), Kasumi-2 ($p = 0.040$; $p = 0.031$), Kasumi-6 ($p = 0.015$; $p = 0.041$), BDCM ($p = 0.013$; $p = 0.037$), and K562 ($p = 0.01$; $p = 0.026$). The Kruskal–Wallis test was used to compare multiple groups, followed by Dunn’s multiple comparison test. The data are presented as a median with an interquartile range (Q1–Q3). The upper and lower lines of each box indicate the 25th (Q1) and 75th (Q3) percentiles. The line inside each box indicates the median. The Kruskal–Wallis H test showed a significant difference in the mRNA expression levels of miR-520a between different groups ($\chi^2(5) = 22.87$, $p = 0.0004$; * $p = 0.027$ for Kasumi-1; * $p = 0.037$ for Kasumi-6; ** $p = 0.001$ for Kasumi-2; ** $p = 0.012$ for BDCM; *** $p = 0.0002$ for K652 cell lines compared to miR-negative control (NC); $n = 3–5$)

Table 3. Real-time quantitative polymerase chain reaction (RT-qPCR) analysis of microRNA (miR)-520a in tissue specimens of acute myeloid leukemia (AML) patients and healthy volunteers

Variables	Healthy volunteers (n = 22)	AML patients (n = 24)
Minimum	0.270	0.250
Q1	1.688	1.108
Median	2.780	1.250
Q3	3.550	1.525
Maximum	4.800	2.500
Mean ranks	30.07	14.93
Mann–Whitney U	75.5	
p-value	<0.001*	

* $p < 0.001$ compared to miR-52a expression analysis in healthy volunteers; Q1 – 1st quartile; Q3 – 3rd quartile. The Mann–Whitney U test was used to compare the 2 groups.

multiple comparison tests; $\chi^2(5) = 22.87$). The K562 cells possessed the lowest expression values ($p = 0.0002$) among all cancer cell lines and were therefore selected for further characterization. Therefore, the results showed that miR-520a was negatively regulated in AML and may play a prognostic role in this malignancy.

Overexpression of miR-520a decreases proliferation and viability

To examine the function of miR-520a in AML, miR-520a was overexpressed in K562 cells, and its overexpression was confirmed by real-time PCR (Fig. 2A, Table 5; $p = 0.0006$; Mann–Whitney test, $U = 0$). An MTT assay was used to investigate the proliferative impact of miR-520a impact on AML. The miR-520a-overexpressing K562 leukemia cells were found to exhibit significantly lower proliferation rates (Fig. 2B, Table 6; $p = 0.031$; Mann–Whitney test,

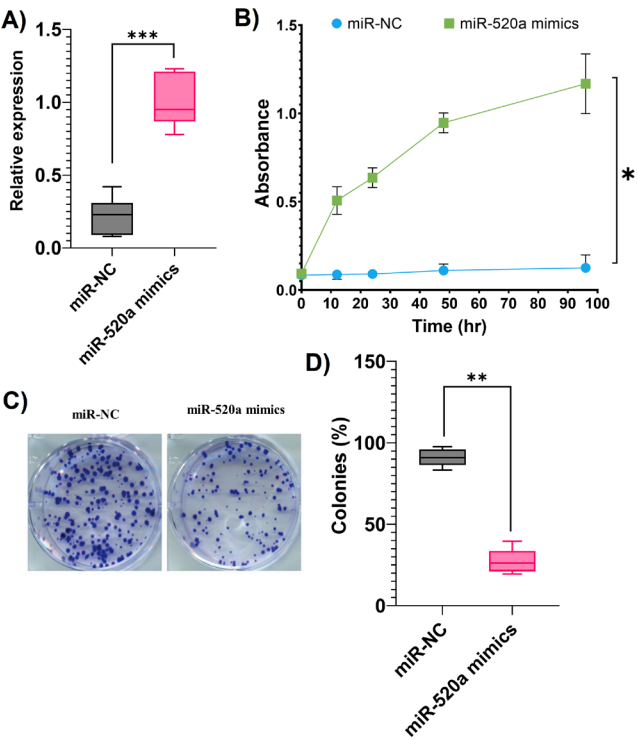


Fig. 2. Overexpression of microRNA (miR)-520a reduces leukemia cell proliferation and viability. **A.** Relative gene expression of miR-520a in miR-negative control (NC) or miR-520a mimics-transfected K562 cells. The data were not normally distributed and were tested by the Shapiro–Wilk test and Kolmogorov–Smirnov test with p-values for miR-NC ($p = 0.013$; $p = 0.021$) and miR-520a ($p = 0.036$; $p = 0.047$). The Mann–Whitney U test was used to compare the 2 groups. The data are presented as a median with an interquartile range (Q1–Q3). The upper and lower lines of each box indicate the 25th (Q1) and 75th (Q3) percentiles. The line inside each box indicates the median; **B.** MTT assay for proliferation analysis of miR-NC or miR-520a mimics-transfected K562 cells. The data were not normally distributed and were tested by the Shapiro–Wilk test and Kolmogorov–Smirnov test with p-values for miR-NC ($p = 0.014$; $p = 0.032$) and miR-520a ($p = 0.034$; $p = 0.027$), indicating significant difference at time intervals. The Mann–Whitney test was used to compare the 2 groups. The data are presented as a median with an interquartile range (Q1–Q3); **C.** Colony forming assay for viability analysis of miR-NC or miR-520a mimics-transfected K562 cells; **D.** Percentage number of colonies formed by miR-NC or miR-520a mimics-transfected K562 cells. The data were not normally distributed and were tested by the Shapiro–Wilk test and Kolmogorov–Smirnov test with p-values for miR-NC ($p = 0.01$; $p = 0.031$) and miR-520a ($p = 0.015$; $p = 0.025$). The upper and lower lines of each box indicate the 25th (Q1) and 75th (Q3) percentiles. The line inside each box indicates the median. The Mann–Whitney test was used to compare the 2 groups. The data are presented as a median with an interquartile range (Q1–Q3) ($n = 3–5$)

*** $p = 0.0006$; * $p = 0.031$; ** $p = 0.002$ compared to miR-NC.

Table 4. Real-time quantitative polymerase chain reaction (RT-qPCR) analysis in normal myeloid cells (NCI-H5N6) and various myeloid cancerous cell lines

Variables	NCI-H526	Kasumi-1	Kasumi-2	Kasumi-6	BDCM	K562
Minimum	0.8700	0.2700	0.2200	0.3300	0.2200	0.2200
Q1	1.400	0.3400	0.2600	0.4100	0.3500	0.2700
Median	1.500	0.5200	0.4400	0.5100	0.4600	0.3200
Q3	2.130	0.6500	0.5000	0.6400	0.5400	0.3900
Maximum	2.490	0.7700	0.6200	0.6600	0.6700	0.4700
Mean ranks	39.00	23.14	15.71	22.43	19.14	9.571
Mean rank difference	–	15.86	23.29	16.57	19.86	29.43
Kruskal–Wallis statistic	$\chi^2(5) = 22.87$; $p = 0.0004$					
Dunn's multiple comparison test (p-value)	–	0.027*	0.001**	0.037*	0.012*	0.001***

* $p = 0.027$ for Kasumi-1; * $p = 0.037$ for Kasumi-6; ** $p = 0.001$ for Kasumi-2; ** $p = 0.012$ for BDCM; *** $p = 0.0002$ for K562 cell lines compared to NCI-H526; Q1 – 1st quartile; Q3 – 3rd quartile. The Kruskal–Wallis test was performed, followed by Dunn's multiple comparison test to compare the multiple groups.

Table 5. Relative gene expression of microRNA (miR)-520a in miR-negative control (NC) or miR-520a mimics-transfected K562 cells and the percentage number of colonies

Variables	Groups			
	A		B	
	miR-NC	miR-520a mimics	miR-NC (%)	miR-520a mimics (%)
Minimum	0.08000	0.7800	83.30	19.40
Q1	0.09000	0.8700	86.45	21.13
Median	0.2300	0.9500	90.95	26.20
Q3	0.3100	1.210	95.95	33.75
Maximum	0.4200	1.230	97.60	39.60
Mean ranks	4.000	11.00	9.500	3.500
Mann–Whitney U	0		0	
p-value	0.001***		0.002**	

A. Relative gene expression of miR-520a in miR-NC or miR-520a mimics-transfected K562 cells. The Mann–Whitney test was used to compared the 2 groups ($n = 3-5$); B. Percent number of colonies formed by miR-NC or miR-520a mimics-transfected K562 cells. The Mann–Whitney test was used to compare the 2 groups ($n = 3-5$); *** $p = 0.001$ (compared to miR-NC); Q1 – 1st quartile; Q3 – 3rd quartile.

$U = 2$). The viability of K562 cancer cells was negatively affected by miR-520a. Cancer cells transfected with miR-520a mimics showed markedly lower colony formation potential compared to normal cells transfected with miR-NC (Fig. 2C, Table 5; $p = 0.002$; Mann–Whitney test, $U = 0$). These findings demonstrate that miR-520a negatively regulates cancer cell proliferation in AML, indicating its anticancer therapeutic potential (Fig. 2D).

Overexpression of miR-520a induces apoptosis in leukemia cells

Evaluation of the nuclear morphology of K562 leukemia cells using the AO/EB staining method showed that cancer cells exhibit a loss of nuclear viability when transfected with miR-520a mimics (Fig. 3A,B, Table 7; $p = 0.002$; Mann–Whitney test, $U = 0$). Consistent with these findings, Annexin V-FITC/PI dual staining revealed that K562 cells transfected with miR-520a mimics demonstrated apoptotic cell death (Fig. 3C,D, Table 7; $p = 0.002$; Mann–Whitney test, $U = 0$). Moreover, the expression of Bax

Table 6. MTT assay for proliferation analysis of microRNA-negative control (miR-NC) or miR-520a mimics-transfected K562 cells

Variables	miR-NC	miR-520a mimics
Minimum	0.084	0.091
Q1	0.086	0.295
Median	0.091	0.623
Q3	0.118	1.071
Maximum	0.126	1.181
Lower 95% CI	0.077	0.147
Upper 95% CI	0.122	1.195
Mann–Whitney U	2	
p-value	0.031*	

* $p = 0.0317$ compared to miR-NC; Q1 – 1st quartile; Q3 – 3rd quartile; 95% CI – 95% confidence interval. The Mann–Whitney test was used to compare the 2 groups ($n = 3-5$ for both groups).

was found to increase, while Bcl-2 protein expression decreased due to the overexpression of miR-520a, which acts as a positive signal for the induction of apoptosis (Fig. 4A, Table 8; $p = 0.002$; Mann–Whitney test, $U = 0$). Together,

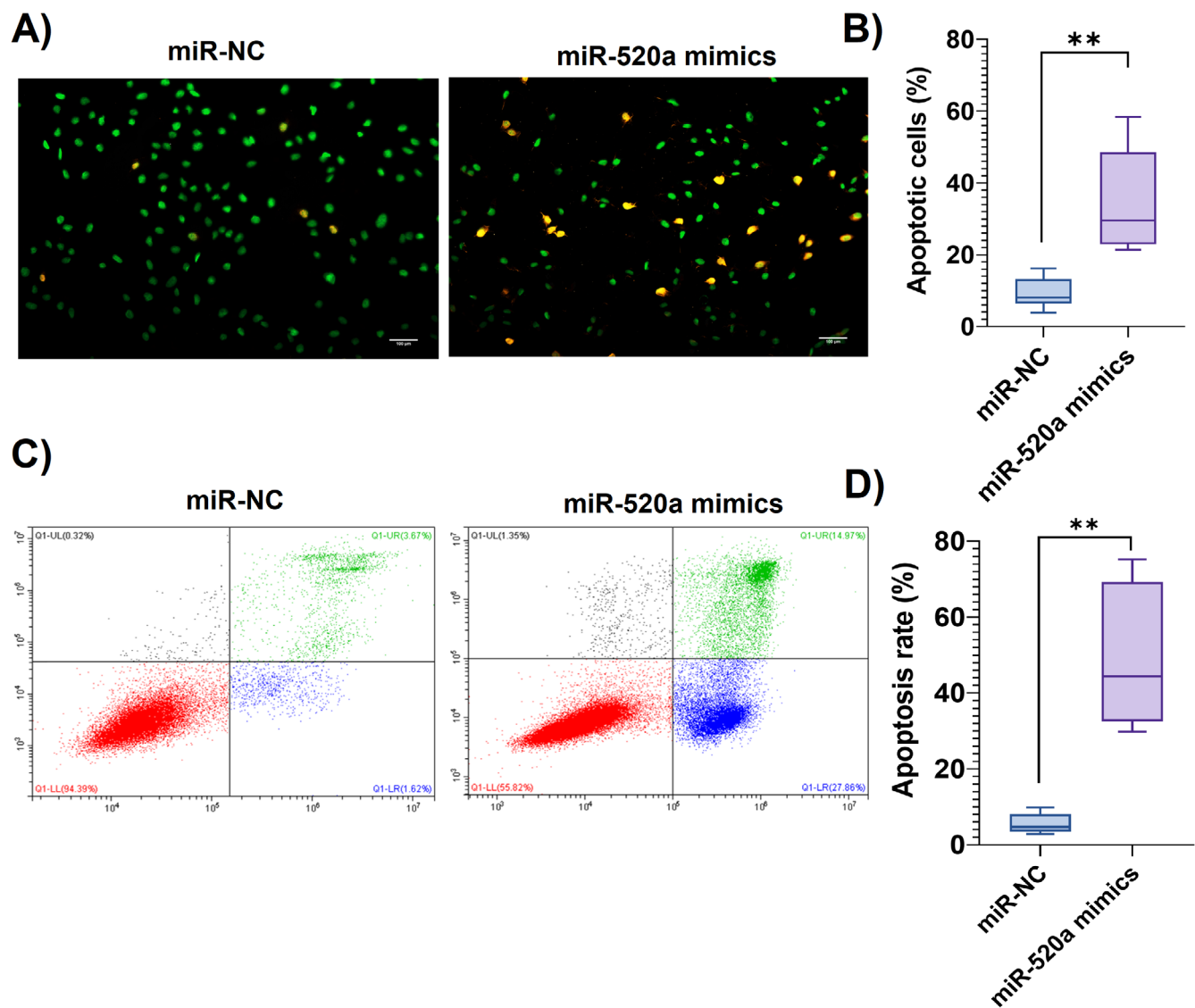


Fig. 3. Overexpression of microRNA (miR)-520a induces apoptosis in leukemia cells. **A.** Acridine orange/ethidium bromide (AO/EB) staining for the analysis of nuclear morphology of miR-negative control (NC) or miR-520a mimics-transfected K562 cells; **B.** Quantification of the percentage of apoptotic cells based on nuclear morphology in miR-NC and miR-520a mimics-transfected K562 cells. The data were not normally distributed and were tested by the Shapiro–Wilk test and Kolmogorov–Smirnov test with p-values for miR-NC ($p = 0.011$; $p = 0.021$) and miR-520a ($p = 0.022$; $p = 0.036$). The Mann–Whitney test was used to compare the 2 groups. The data are presented as a median with an interquartile range (Q1–Q3). The upper and lower lines of each box indicate the 25th (Q1) and 75th (Q3) percentiles. The line inside each box indicates the median; **C.** Flow cytometry-based analysis of apoptosis of miR-NC or miR-520a mimics-transfected K562 cells stained with Annexin V-fluorescein isothiocyanate (FITC)/propidium iodide (PI) dual staining mix; **D.** Quantification of the percentage rate of apoptosis of miR-NC or miR-520a mimics-transfected K562 cells based on flow cytometry analysis. The data were not normally distributed and were tested by the Shapiro–Wilk test and Kolmogorov–Smirnov test with p-values for miR-NC ($p = 0.029$; $p = 0.028$) and miR-520a ($p = 0.034$; $p = 0.017$). The Mann–Whitney test was used to compare the 2 groups. The data are presented as a median with an interquartile range (Q1–Q3). The upper and lower lines of each box indicate the 25th (Q1) and 75th (Q3) percentiles. The line inside each box indicates the median ($n = 3–5$)

** $p = 0.002$ compared to miR-NC.

the findings support our hypothesis that miR-520a positively regulates cancer cell apoptosis in AML, further confirming its anticancer therapeutic potential against this disorder.

miR-520a targets the PI/AKT signaling pathway in AML

To find a possible mechanism for the regulatory role of miR-520a in AML, we performed western blotting for

both AKT and PI3K proteins (non-phosphorylated and phosphorylated). The overexpression of miR-520a did not significantly affect non-phosphorylated PI3K and AKT protein levels. However, a substantial decrease in the expression levels of the phosphorylated AKT and PI3K (p-AKT and p-PI3K) was observed due to the overexpression of miR-520a (Fig. 4A–D, Table 8; $p = 0.002$; Mann–Whitney test, $U = 0$). This indicates that miR-520a targets and blocks the PI3K/AKT signaling pathway in AML to exert its anti-proliferative role.

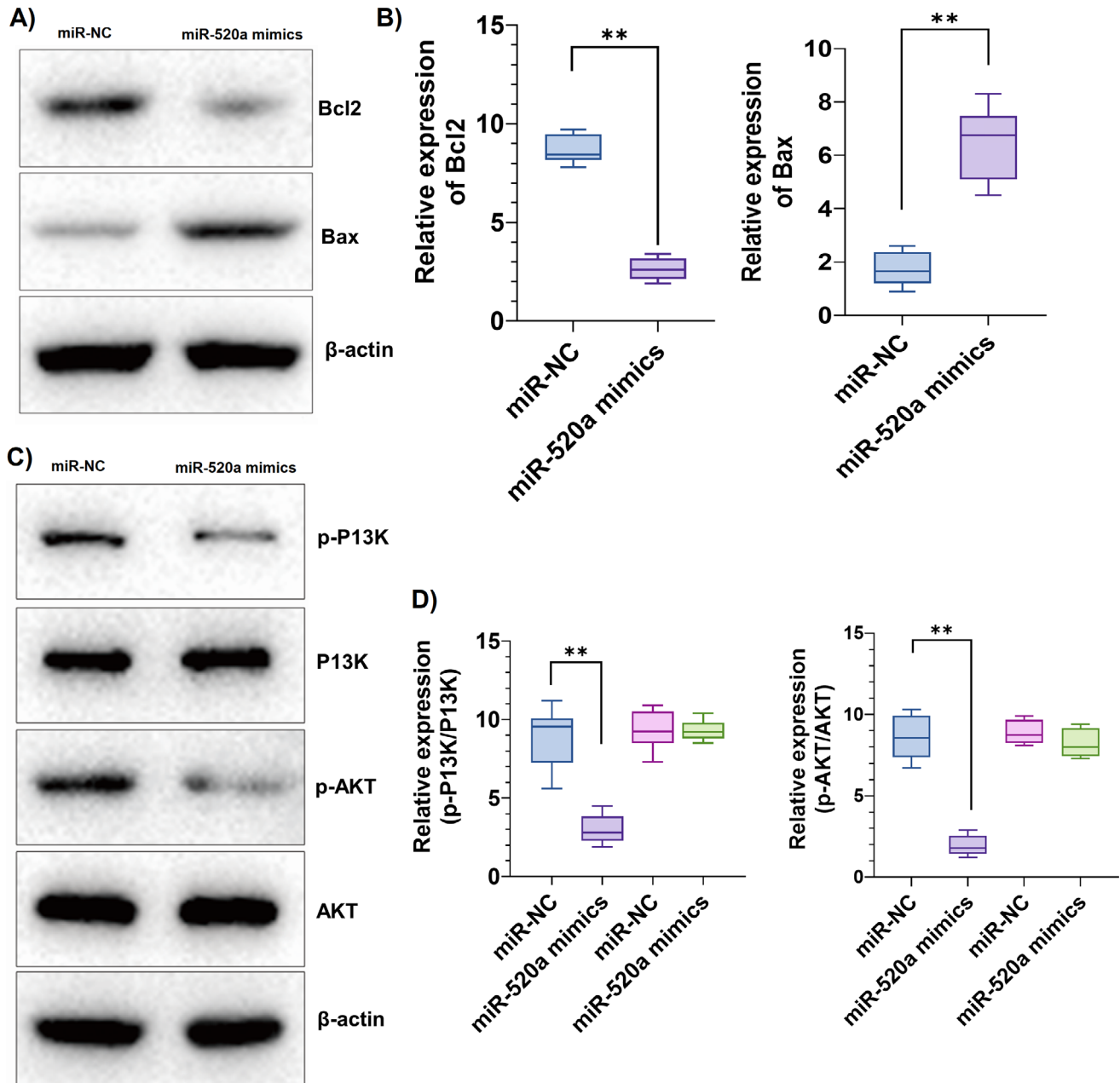


Fig. 4. MicroRNA (miR)-520a targets the PI3K/AKT signaling pathway in acute myeloid leukemia (AML). A. Western blotting of Bax and Bcl-2 proteins from miR-negative control (NC) or miR-520a mimics-transfected K562 cells using β -actin protein as an internal control; B. Relative protein expression levels of Bax and Bcl-2 proteins from miR-NC or miR-520a mimics-transfected K562 cells. The data were not normally distributed and were tested by the Shapiro–Wilk test and Kolmogorov–Smirnov test with p-values for miR-NC (Bax: $p = 0.017$; $p = 0.037$, Bcl2: $p = 0.047$; $p = 0.021$) and miR-520a (Bax: $p = 0.015$; $p = 0.034$, Bcl2: $p = 0.019$; $p = 0.042$). The Mann–Whitney test was used to compare the 2 groups. The data are presented as a median with an interquartile range (Q1–Q3). The upper and lower lines of each box indicate the 25th (Q1) and 75th (Q3) percentiles. The line inside each box indicates the median; C. Western blotting of phosphorylated (p)-PI3K, PI3K, p-AKT, and AKT proteins from miR-NC or miR-520a mimics-transfected K562 cells using β -actin protein as internal control; D. Relative protein expression levels of p-PI3K, PI3K, p-AKT, and AKT proteins from miR-NC or miR-520a mimics-transfected K562 cells. The data were not normally distributed and were tested by the Shapiro–Wilk test and Kolmogorov–Smirnov test with p-values for miR-NC (p-PI3K: $p = 0.043$; $p = 0.021$, PI3K: $p = 0.018$; $p = 0.015$, p-AKT: $p = 0.037$; $p = 0.027$, AKT: $p = 0.035$; $p = 0.026$) and miR-520a (p-PI3K: $p = 0.025$; $p = 0.038$, PI3K: $p = 0.036$; $p = 0.021$, p-AKT: $p = 0.016$; $p = 0.014$, AKT: $p = 0.021$; $p = 0.019$). The Mann–Whitney test was used to compare the 2 groups. The data are presented as a median with an interquartile range (Q1–Q3). The upper and lower lines of each box indicate the 25th (Q1) and 75th (Q3) percentiles. The line inside each box indicates the median ($n = 3–5$)

** $p = 0.002$ compared to miR-NC.

Discussion

Recently, miRs have been found to be crucial regulatory molecules in almost all eukaryotic organisms.¹⁷ They are seen to influence many developmental and physiological

processes in humans,¹⁸ such as proliferation, differentiation, programmed cell death, and apoptosis.¹⁹ MicroRNAs exert their regulatory role through post-transcriptional silencing of target protein-coding genes.²⁰ Dysregulation of many miRs has been associated with various cancers, prompting

Table 7. Quantification of the percentage of apoptotic cells in microRNA-negative control (miR-NC) and miR-520a mimics-transfected K562 cells based on nuclear morphology and flow cytometry analysis

Variables	Groups			
	A		B	
	miR-NC	miR-520a mimics	miR-NC	miR-520a mimics
Minimum	3.900	21.40	2.900	29.80
Q1	6.450	22.90	3.500	32.50
Median	8.100	29.55	4.700	44.45
Q3	13.28	48.50	8.075	69.28
Maximum	16.20	58.40	9.800	75.20
Mann–Whitney U	0		0	
p-value	–	0.002**	–	0.002**

A. Quantification of the percentage of apoptotic cells based on nuclear morphology in miR-NC and miR-520a mimics-transfected K562 cells. The Mann–Whitney test was used to compare the 2 groups. The data are presented as median with interquartile range (Q1–Q3); B. Quantification of the percentage rate of apoptosis of miR-NC or miR-520a mimics-transfected K562 cells based on flow cytometry analysis. The Mann–Whitney test was used to compare the 2 groups; **p = 0.002 compared to miR-NC; Q1 – 1st quartile; Q3 – 3rd quartile.

Table 8. MicroRNA (miR)-520a targets the PI3K/AKT signaling pathway in acute myeloid leukemia (AML) with protein expression levels of Bax and Bcl-2, phosphorylated (p)-PI3K, PI3K, p-AKT, and AKT

Variables	Groups											
	A. Bax		B. Bcl2		C. p-PI3K		D. PI3K		E. p-AKT		F. AKT	
	miR-NC	miR-520a mimics	miR-NC	miR-520a mimics	miR-NC	miR-520a mimics	miR-NC	miR-520a mimics	miR-NC	miR-520a mimics	miR-NC	miR-520a mimics
Minimum	0.9000	4.500	7.800	2.200	5.600	1.900	7.300	8.500	6.700	1.200	8.100	7.300
Q1	1.200	5.100	8.175	2.200	7.250	2.275	8.500	8.800	7.375	1.425	8.250	7.450
Median	1.650	6.750	8.450	2.600	9.550	2.800	9.250	9.200	8.550	1.800	8.750	8.000
Q3	2.375	7.475	9.475	3.175	10.08	3.825	10.53	9.800	9.925	2.525	9.675	9.175
Maximum	2.600	8.300	9.700	3.400	11.20	4.500	10.90	10.40	10.30	2.900	9.900	9.400
Mann–Whitney U	0		0		0		16.50		0		9	
p-value	0.002**		0.002**		0.002**		0.855		0.002**		0.179	

A,B. Relative protein expression levels of Bax and Bcl-2 proteins from miR-negative control (NC) or miR-520a mimics-transfected K562 cells. The Mann–Whitney test was used to compare the 2 groups (n = 6 for both groups); C–F. Relative protein expression levels of p-PI3K, PI3K, p-AKT, and AKT proteins from miR-NC or miR-520a mimics-transfected K562 cells (n = 3–5 for both groups); **p = 0.002 compared to miR-NC; Q1 – 1st quartile; Q3 – 3rd quartile.

researchers to investigate their regulatory role in malignancy.²¹ MicroRNAs are also important prognostic markers for human cancer.²² Moreover, the dysregulation of miRs has been reported in AML.²³ In a recent report, miR-98 was highly expressed in AML, and the study findings were helpful in determining the prognostic importance of miR biomolecules.²⁴ The *miR-520a* is a tumor suppressor gene in many human cancers,^{25,19} and its downregulation has been associated with human breast cancer.²⁶ In the present investigation, we found a similar dysregulation of miR-520a in AML. Previously, the upregulation of miR-520a was shown to negatively affect cancer cell proliferation,²⁷ which is supported by our results showing that the overexpression of miR-520a decreases AML cell proliferation.

Furthermore, we found that the reason behind the decrease in leukemia cell proliferation under miR-520a overexpression was the induction of apoptotic cell death in leukemia cells. Similar conclusions were drawn from previous research studies.¹¹ The PI3K/AKT signaling pathway has

shown involvement in the regulation of cell proliferation and apoptosis.²⁸ The abnormal activation of this pathway is coupled with increased cell proliferation and survival of cells in many human cancers.²⁹ Furthermore, it is important to highlight that phosphorylation of the PI3K and AKT proteins is responsible for stimulating the PI3K/AKT signaling pathway.²⁸

Interestingly, the overexpression of miR-520a in leukemia cells considerably decreased the levels of phosphorylated AKT and PI3K proteins. This indicates that miR-520a inhibits the phosphorylation of these proteins and blocks the PI3K/AKT signaling cascade, leading to decreased proliferation of leukemia cells and the initiation of apoptosis. A similar mechanism of miR-520a has been reported previously.²⁵ In summary, the current study explored the possibility of using the drug-based targeting of miR-520a for its transcriptional enhancement, as an alternative anticancer approach that could be investigated in the future against human AML.

Limitations

There were 3 limitations to this study. First, a limited number of cell lines were used in the present study to examine the effects of miR-520a. Second, inhibitors of miR-52a are not investigated in the present study. Third, other than PI3K/AKT, other significant signaling mechanisms are not explored in the current study.

Conclusions

The results of the present research established the mechanism by which miR-520a regulates the progression of human AML. The study also revealed the tumor-suppressing role of miR-520a in AML, which can be amplified by activating the PI3K/AKT pathway that specifically targets regulatory molecules to prevent proliferation of human AML efficiently.

Supplementary files

The Supplementary materials are available at <https://doi.org/10.5281/zenodo.8297073>. The package contains the following files:

Supplementary Fig. 1. Uncropped images of Western blots illustrated in Fig. 1.

ORCID iDs

Jing Xiao  <https://orcid.org/0009-0001-1866-1638>
 Fang Wan  <https://orcid.org/0009-0005-2874-5324>
 Lin Tian  <https://orcid.org/0009-0002-7888-4857>
 Yao Li  <https://orcid.org/0009-0009-5394-2441>

References

- Gramates MM, Rabin KR. The adolescent and young adult with cancer. State of the art: Acute leukemias. *Curr Oncol Rep*. 2013;15(4):317–324. doi:10.1007/s11912-013-0325-5
- Santini V, Lübbert M, Wierzbowska A, Ossenkoppele GJ. The clinical value of decitabine monotherapy in patients with acute myeloid leukemia. *Adv Ther*. 2022;39(4):1474–1488. doi:10.1007/s12325-021-01948-8
- Khadka S, Solanki D, Singh J, et al. Trends and outcomes of venous thromboembolism in adult hospitalizations with acute myeloid leukemia: Analysis of nationwide inpatient sample from 2010 to 2014. *Postgrad Med*. 2021;133(2):160–165. doi:10.1080/00325481.2020.1863717
- Guo S, Li B, Chen Y, et al. Hsa_circ_0012152 and Hsa_circ_0001857 accurately discriminate acute lymphoblastic leukemia from acute myeloid leukemia. *Front Oncol*. 2020;10:1655. doi:10.3389/fonc.2020.01655
- Guan J, Liu P, Wang A, Wang B. Long non-coding RNA ZEB2-AS1 affects cell proliferation and apoptosis via the miR-122-5p/PLK1 axis in acute myeloid leukemia. *Int J Mol Med*. 2020;46(4):1490–1500. doi:10.3892/ijmm.2020.4683
- Li ZJ, Cheng J, Song Y, Li HH, Zheng JF. LncRNA SNHG5 upregulation induced by YY1 contributes to angiogenesis via miR-26b/CTGF/VEGFA axis in acute myelogenous leukemia. *Lab Invest*. 2021;101(3):341–352. doi:10.1038/s41374-020-00519-9
- Koenig KL, Sahasrabudhe KD, Sigmund AM, Bhatnagar B. AML with myelodysplasia-related changes: Development, challenges and treatment advances. *Genes (Basel)*. 2020;11(8):845. doi:10.3390/genes11080845
- Bernasconi P, Borsani O. Targeting leukemia stem cell-niche dynamics: A new challenge in AML treatment. *J Oncol*. 2019;2019:8323592. doi:10.1155/2019/8323592
- Wallace JA, O'Connell RM. MicroRNAs and acute myeloid leukemia: Therapeutic implications and emerging concepts. *Blood*. 2017;130(11):1290–1301. doi:10.1182/blood-2016-10-697698
- Wang L, Wang Y, Lin J. MiR-152-3p promotes the development of chronic myeloid leukemia by inhibiting p27. *Eur Rev Med Pharmacol Sci*. 2018;22(24):8789–8796. doi:10.26355/eurrev_201812_16646
- Yu J, Tan Q, Deng B, Fang C, Qi D, Wang R. The microRNA-520a-3p inhibits proliferation, apoptosis and metastasis by targeting MAP3K2 in non-small cell lung cancer. *Am J Cancer Res*. 2015;5(2):802–811. PMID:25973317. PMCID:PMC4396038.
- Xie Y, Xue C, Guo S, Yang L. MicroRNA-520a suppresses pathogenesis and progression of non-small-cell lung cancer through targeting the RRM2/Wnt axis. *Anal Cell Pathol (Amst)*. 2021;2021:9652420. doi:10.1155/2021/9652420
- Hong S, Chen S, Wang X, et al. ATAD2 silencing decreases VEGFA secretion through targeting has-miR-520a to inhibit angiogenesis in colorectal cancer. *Biochem Cell Biol*. 2018;96(6):761–768. doi:10.1139/bcb-2018-0081
- Wang X, Wang P, Zhu Y, Zhang Z, Zhang J, Wang H. MicroRNA-520a attenuates proliferation of Raji cells through inhibition of AKT1/NF-κB and PERK/eIF2α signaling pathway. *Oncol Rep*. 2016;36(3):1702–1708. doi:10.3892/or.2016.4975
- Holland M, Cunningham R, Seymour L, et al. Separation, banking, and quality control of peripheral blood mononuclear cells from whole blood of melanoma patients. *Cell Tissue Bank*. 2018;19(4):783–790. doi:10.1007/s10561-018-9734-x
- Chen XY, Qin XH, Xie XL, Liao CX, Liu DT, Li GW. Overexpression miR-520a-3p inhibits acute myeloid leukemia progression via targeting MUC1. *Transl Oncol*. 2022;22:101432. doi:10.1016/j.tranon.2022.101432
- He L, Hannon GJ. MicroRNAs: Small RNAs with a big role in gene regulation. *Nat Rev Genet*. 2004;5(7):522–531. doi:10.1038/nrg1379
- Chang TC, Mendell JT. microRNAs in vertebrate physiology and human disease. *Annu Rev Genom Hum Genet*. 2007;8(1):215–239. doi:10.1146/annurev.genom.8.080706.092351
- Su H, Ren F, Jiang H, Chen Y, Fan X. Upregulation of microRNA-520a-3p inhibits the proliferation, migration and invasion via spindle and kinetochore associated 2 in gastric cancer. *Oncol Lett*. 2019;18(3):3323–3330. doi:10.3892/ol.2019.10663
- Patil VS, Zhou R, Rana TM. Gene regulation by non-coding RNAs. *Crit Rev Biochem Mol Biol*. 2014;49(1):16–32. doi:10.3109/10409238.2013.844092
- Bhatti I, Lee A, Lund J, Larvin M. Small RNA: A large contributor to carcinogenesis? *J Gastrointest Surg*. 2009;13(7):1379–1388. doi:10.1007/s11605-009-0887-6
- Lan H, Lu H, Wang X, Jin H. MicroRNAs as potential biomarkers in cancer: Opportunities and challenges. *Biomed Res Int*. 2015;2015:125094. doi:10.1155/2015/125094
- Barrera-Ramirez J, Lavoie JR, Maganti HB, et al. Micro-RNA profiling of exosomes from marrow-derived mesenchymal stromal cells in patients with acute myeloid leukemia: Implications in leukemogenesis. *Stem Cell Rev Rep*. 2017;13(6):817–825. doi:10.1007/s12015-017-9762-0
- Hu N, Cheng Z, Pang Y, et al. High expression of MiR-98 is a good prognostic factor in acute myeloid leukemia patients treated with chemotherapy alone. *J Cancer*. 2019;10(1):178–185. doi:10.7150/jca.26391
- Lv X, Li CY, Han P, Xu XY. MicroRNA-520a-3p inhibits cell growth and metastasis of non-small cell lung cancer through PI3K/AKT/mTOR signaling pathway. *Eur Rev Med Pharmacol Sci*. 2018;22(8):2321–2327. doi:10.26355/eurrev_201804_14822
- Mu J, Ning S, Wang X, et al. The repressive effect of miR-520a on NF-κB/IL-6/STAT-3 signal involved in the glabridin-induced anti-angiogenesis in human breast cancer cells. *RSC Adv*. 2015;5(43):34257–34264. doi:10.1039/C4RA17062H
- Zhang R, Liu R, Liu C, et al. A novel role for MiR-520a-3p in regulating EGFR expression in colorectal cancer. *Cell Physiol Biochem*. 2017;42(4):1559–1574. doi:10.1159/000479397
- Chang F, Lee JT, Navolanic PM, et al. Involvement of PI3K/Akt pathway in cell cycle progression, apoptosis, and neoplastic transformation: A target for cancer chemotherapy. *Leukemia*. 2003;17(3):590–603. doi:10.1038/sj.leu.2402824
- Vara JÁF, Casado E, De Castro J, Cejas P, Belda-Iniesta C, González-Barón M. PI3K/Akt signalling pathway and cancer. *Cancer Treat Rev*. 2004;30(2):193–204. doi:10.1016/j.ctrv.2003.07.007